LANGMUIR Article
Cite This: Langmuir 2019, 35, 9979−9987
pubs.acs.org/Langmuir

# Coalescence-Induced Swift Jumping of Nanodroplets on Curved Surfaces

Xukun He,[†] Lei Zhao,[†] and Jiangtao Cheng*

Department of Mechanical Engineering, Virginia Tech, Blacksburg, Virginia 24061, United States

Supporting Information

**ABSTRACT:** In this work, we use molecular dynamics simulations to investigate coalescence-induced jumping of nanodroplets on curved surfaces with different wettabilities. On a curved surface, a liquid bridge will first form between two coalescing droplets as on a flat surface. However, contrary to symmetry-breaking-induced jumping on a flat surface, coalescing droplets would jump earlier than the liquid bridge gets into contact with the curved surface. Such an early symmetry breaking is induced by the opposite motion of coalescing droplets along the lateral direction on the curved surface. We find that surface curvature can effectively facilitate the jumping of coalescing nanodroplets via enhanced symmetry breaking. The energy conversion efficiency is improved from ∼0.15% on a flat surface to ∼2.9% on a curved surface, which is about 20 times enhancement. In addition, we conducted an energy scaling analysis by considering the lumped effects of both viscous dissipation and contact line friction on the jumping behaviors. We conclude that curvature-enhanced jumping in the nanoscale can be ascribed to the mitigated contact line dissipation $E_{cl}$, whereas viscous dissipation $E_{vis}$ is maintained almost at the same level. Therefore, we unveil a scaling law between the energy conversion efficiency $\eta$ on surfaces with different curvatures and the product of contact line length and contact time. Interestingly, the increasing surface curvature could allow the occurrence of coalescence-induced jumping on a less superhydrophobic surface. Hence, a phase map of coalescence-induced jumping in terms of surface curvature ratio and surface wettability is presented. Essentially, the paradigm of curved surfaces in the nanoscale used in this study is characteristic of the topography of micro/nanostructured surfaces, on which coalescence-induced droplet jumping has been experimentally observed. This work justifies the critical role of nanoroughness in boosting coalescence-induced jumping of nanodroplets and sheds light on the passive control of nanodroplets jumping on functional surfaces.

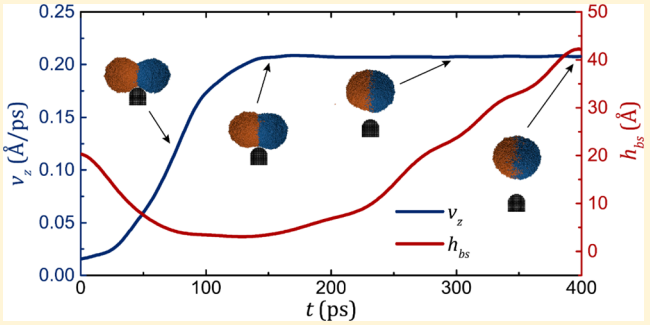


## 1. INTRODUCTION

When two droplets on a surface begin coalescing, the released surface energy from coalescence would drive the coalescing droplet to jump off the surface. This intriguing phenomenon was first observed during dropwise condensation on a superhydrophobic surface, which is then termed as "coalescence-induced jumping".[1−5] This self-propelled jumping behavior provides us a passive approach to droplet control, which has been utilized not only in enhancing phase-change heat transfer[6,7] but also in several other applications including self-cleaning,[3] anti-icing,[8,9] and energy harvesting.[10,11]

To promote and employ the jumping behavior of coalescing droplets in practical applications, two prominent standards are desired. One standard is coalescence-induced jumping occurring at a smaller length scale,[12] ideally in the nanoscale; and the other standard is coalesced droplet jumping with higher velocities even on more wettable surfaces. Previous studies[4,13] showed that it is technically demanding to have both of these requirements satisfied at the same time because the jumping velocities of smaller coalescing droplets would be significantly depressed because of the even higher level of energy dissipation, which may lead to no jumping of nanodroplets. However, in a recent experimental study,[12] the coalescence-induced jumping of nanodroplets of ∼500 nm in diameter were observed on carbon nanotube-decorated superhydrophobic surfaces. Several numerical studies using molecular dynamics (MD) simulations[14−17] also concluded that certain coalescing nanodroplets could successfully jump off superhydrophobic surfaces.

Even though the first standard can be relatively easily satisfied by decreasing the characteristic length of surface roughness and increasing the apparent advancing contact angle on a textured surface,[12] the jumping velocity of nanodroplets can still be impeded in that the efficiency of converting surface energy to kinetic energy in the nanoscale drops abruptly to only ∼1%,[15,16] which is a significant reduction compared with that of ∼5% in the microscale.[2,12] To break the jumping velocity limit because of this low energy conversion efficiency,

Received: May 2, 2019
Revised: June 24, 2019
Published: July 6, 2019






DOI: 10.1021/acs.langmuir.9b01300
Langmuir 2019, 35, 9979−9987

surfaces decorated with micro/nanoridges[17−19] were already introduced to improve the energy conversion efficiency through inducing the early liquid-bridge impact on the structured surfaces. However, the existence of micro/nanoridges would inevitably increase the liquid−solid contact area, incurring larger adhesive force and restricting their applications only on the almost nonwetting surfaces. Therefore, an alternative jumping enhancement method utilizing intrinsic surface curvature was proposed to alleviate the liquid−solid contact.[20] In this respect, the coalescence-induced jumping of microdroplets has been successfully observed on the rounded hydrophobic microfibers,[20−22] which at least partly validated the efficacy of the curvature-enhanced jumping in the macro/microscale. Hence, it is reasonable to expect surface curvature in the nanoscale could facilitate nanodroplet jumping, meeting both the jumping standards, that is, in a smaller scale and energy-effective, in the meantime. Furthermore, contact line friction[23−25] becomes a non-negligible source of energy dissipation in the nanoscale, necessitating the consideration of contact line dissipation in the energy efficiency analysis of coalescence-induced nanodroplet jumping.

In this work, we use MD simulations to study the enhanced jumping of coalescing nanodroplets on curved surfaces. First, the dynamics of coalescence-induced jumping of nanodroplets on a cylindrical surface are investigated. Different from the jumping behavior on a flat surface, the coalesced droplet on a curved surface could achieve early jumping and early acceleration upon coalescence. Following a greatly mitigated deceleration process during the detachment of the to-be-jumping droplet, the coalesced droplet successfully jumps off the surface with a higher velocity. Next, by conducting a scaling analysis of energy dissipation including the effect of contact line friction, we elucidate the energy conversion efficiency of coalescence-induced jumping in the nanoscale. We find that the reduction of contact line dissipation plays a dominant role over viscous dissipation in improving energy conversion efficiency on curved surfaces. As expected, the requirement on surface hydrophobicity for droplet jumping decreases with increasing surface curvature so that enhanced jumping on less superhydrophobic surfaces becomes possible in the nanoscale. The paradigm of curved surfaces in this MD study actually characterizes the surface topography with roughness in the nanoscale or microscale, on which coalescence-induced droplet jumping has been experimentally validated. The physical insights gained from this work could clarify the mechanism of curvature-enhanced jumping and pinpoint a potential way to passively control the dynamic behaviors of droplets in the nanoscale.

## 2. MODEL AND METHODS

**2.1. Numerical Method.** All the MD simulations in this work were carried out using the open source code LAMMPS.[26] The simulation domain consists of a solid substrate and two spherical nanodroplets. In this study, the solid substrate is either atomically smooth (Figure 1a) or curved (Figure 1b) to mimic the surface of a nanofiber or a nanotube. To investigate the effect of surface curvature, the radius $R$ of the nanofiber is adjustable, whereas the radius $r$ of the nanodroplets is fixed at 5 nm. In this work, the nondimensional curvature $\varphi = r/R$ was set at 0 (flat surface), 0.25, 1, and 2, respectively, to tune the surface curvature. In the MD simulations, each spherical droplet contains 34916 SPC/E water molecules and the solid substrate is composed of (100) face-centered cubic gold lattices with a lattice constant of 4.08 Å. The two nanodroplets were initially placed 0.5 nm away from each other on the modeled surfaces.

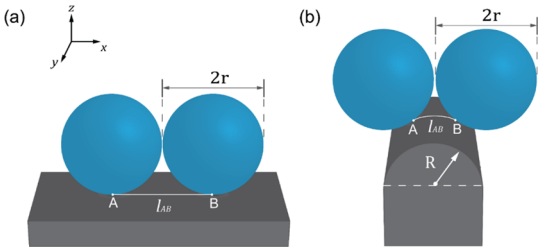


**Figure 1.** Initial configurations of the simulation domain used to study the coalescence-induced jumping of nanodroplets on (a) a flat surface and (b) a curved surface. Here, the characteristic length of the contact line $L$ is defined as the geodesic distance between the two original droplet-surface contact points A and B along the surfaces, namely $l_{AB}$. Coalescence-induced lateral movement of nanodroplets is in the $x$ direction and the out-of-plane jumping is in the $z$ direction.

During the simulation, the substrate atoms are fixed at their initial positions and the motion of water molecules is integrated by the Verlet algorithm. The Au−O interaction and O−O interaction are given by the 12-6 Lennard Jones potential

$$E_{ij} = 4\varepsilon_{ij}\left[\left(\frac{\sigma_{ij}}{d}\right)^{12} - \left(\frac{\sigma_{ij}}{d}\right)^{6}\right] \quad \text{with} \quad d < d_c \tag{1}$$

where $\varepsilon_{ij}$ is the depth of the potential well, $\sigma_{ij}$ is the finite distance where the potential equals to zero, $d_c$ is the cutoff distance of 10 Å, $\varepsilon_{ww}$ stands for the O−O interaction between water molecules, and $\varepsilon_{ws}$ denotes the Au−O interaction between water molecules and the solid atoms. In this work, $\varepsilon_{ww}$ is fixed at 0.1553 kJ/mol and the energy parameter ratio $\varepsilon_{ws}/\varepsilon_{ww}$ is adjusted to tune the surface wettability. The long-range Coulombic forces are computed by particle−particle particle mesh approach[27] and are also truncated at 10 Å.

Prior to the production run, the system was first equilibrated with the Nose−Hoover thermostat in an *NVT* ensemble for 100 ps until the temperature of the two nanodroplets approaches a steady value of 298 K. During the equilibration, all the water molecules were fixed via a harmonic potential to avoid the coalescence of the two nanodroplets. Once the equilibration process was finished, the position constraints on water molecules were released and then the system was integrated in the *NVE* ensemble. All the simulations were run for a sufficiently long period until the coalescing droplets could either jump off the surfaces or simply stay on the surface without jumping.

**2.2. Energy Scaling Analysis of Coalescence-Induced Jumping of Nanodroplets.** Jumping of a coalesced liquid droplet is actually driven by the released surface energy $\Delta E_\gamma$ during the coalescence of two smaller droplets.[2,5,13,14] This jumping behavior is resisted by the adhesion work $E_a$ and energy dissipation $E_d$ in a combined manner. Hence, in a two-droplet coalescence system, the final kinetic energy $E_k$ of the jumping droplet could be expressed as

$$E_k = \Delta E_\gamma - E_a - E_d \tag{2}$$

where $E_k$ is the kinetic energy of the merged droplet and it could be calculated as

$$E_k = \frac{4}{3}\rho\pi r^3 v_j^2 \approx \rho r^3 v_j^2 \tag{3}$$

where $\rho$ is the density of water, $r$ is the initial radius of each droplet, and the jumping velocity $v_j$ is defined as the steady center-of-mass velocity after the coalesced droplet detaches from the surface.

First, we study the jumping phenomenon on an ideally superhydrophobic surface with contact angle $\theta \approx 180°$. The excessive surface energy $\Delta E_\gamma$ of two spherical droplets could be estimated as

$$\Delta E_\gamma \approx (2 - (2)^{2/3})4\pi\gamma r^2 \approx \gamma r^2 \tag{4}$$



DOI: 10.1021/acs.langmuir.9b01300
*Langmuir* 2019, 35, 9979−9987

where $\gamma$ is surface tension of water. Although the surface energy of a droplet might vary with its increased surface area incurred by the additional macrotexture,[19] the change of surface energy on curved surfaces in our work could be ignored because of the nearly constant surface area, which will be discussed in section 3.2.

The adhesion energy $E_a$ becomes negligible as $\theta \approx 180°$

$$\Delta E_a = 2\gamma(1 + \cos\theta)A_{ls} \approx 0 \tag{5}$$

where $A_{ls}$ is the contact area of liquid droplet on the solid surface. Indeed, on a superhydrophobic surface with $\varepsilon_{ws}/\varepsilon_{ww} = 0.1$, the ratio of adhesion energy to the total released surface energy is less than 0.2% (see the Supporting Information).

Most of the previous jumping studies assumed the viscous dissipation of bulk liquid $E_{vis}$ as the only source of energy dissipation. However, as the size scale descends to the nanoscale, the effect of contact line dissipation $E_{cl}$ becomes more prominent and cannot be neglected.[24,28,29] Thus, in this work, energy dissipation $E_d$ is composed of viscous dissipation $E_{vis}$ and contact line dissipation $E_{cl}$

$$\Delta E_d = E_{vis} + E_{cl} \tag{6}$$

Viscous dissipation $E_{vis}$ mainly results from fluid convection (or diffusion) during coalescence, which could be estimated as[13]

$$\Delta E_{vis} = 2\int_0^{\tau_{vis}}\int_\Omega \Phi \, d\Omega dt \approx 2\Omega\Phi\tau_{vis} \tag{7}$$

where $\Omega$ is the volume of each droplet, $\tau_{vis}$ is viscous dissipation time, and $\Phi$ is the dissipation function. It has been justified that the lateral motion (in the $x$-direction) of the coalescing droplets dominates the viscous dissipation during coalescence;[13,17] thus, the dissipation function $\Phi$ could be estimated as

$$\Phi \approx \frac{1}{2}\mu\left(\frac{U_x}{r}\right)^2 \tag{8}$$

where $\mu$ is the water viscosity, $U_x$ is the lumped coalescence velocity of droplets in the $x$ direction. The viscous dissipation time $\tau_{vis}$ was previously defined as the time spanning from the onset of coalescence to the jumping of the coalesced droplet.[17] However, especially on a curved surface, the coalescence process, which is the origin of viscous dissipation, might not be synchronized with droplet jumping. Hence, in this work, based on the lateral motion of droplets during coalescence, $\tau_{vis}$ is defined as the whole period of acceleration and deceleration processes of the coalescing droplets in the $x$ direction, which could also be directly obtained from our MD simulations (see section 3).

Substituting eq 8 in to eq 7, the viscous dissipation $E_{vis}$ could be rewritten as

$$E_{vis} \approx \frac{4}{3}\pi\mu U_x^2 r\tau_{vis} \approx \mu U_x^2 r\tau_{vis} \tag{9}$$

The contact line dissipation $E_{cl}$ is determined by the characteristic contact line velocity $u$, the characteristic length of contact line $L$, contact line friction coefficient $\mu_{cl}$, and contact line dissipation time $\tau_{cl}$[23−25,30]

$$E_{cl} \approx \mu_{cl} u^2 L\tau_{cl} \tag{10}$$

where $\mu_{cl}$ could be approximated by water's dynamic viscosity $\mu$.[24,29,31] In the nanoscale, $u$ should be in the same order of magnitude as the average coalescence velocity $U_x$ in the $x$-direction, and contact line dissipation time $\tau_{cl}$ could be defined as the time period spanning from the onset of coalescence to the detachment of the coalesced droplet from the surface. Here, the characteristic length of the contact line $L$ is defined as the geodesic distance between the two initial droplet−surface contact points A and B along the surface, namely $l_{AB}$ in Figure 1. Thus, $L$ could be obtained based on the geometry relationship as

$$L \approx \begin{cases} 2\dfrac{r}{\varphi}\cos^{-1}\dfrac{\varphi}{\sqrt{1+2\varphi}} & \varphi \neq 0 \\ 2r\varphi = 0 & \varphi = 0 \end{cases} \tag{11}$$

Therefore, the contact line dissipation $E_{cl}$ could be scaled as

$$E_{cl} \approx \mu U_x^2 L\tau_{cl} \tag{12}$$

Combining eqs 3−5, 9, and 12 together, the final jumping velocity could be estimated as

$$v_j^2 \approx \frac{\gamma}{\rho r} - \frac{\mu U_x^2}{\rho r^2}\left(\tau_{vis} + \frac{L}{r}\tau_{cl}\right) \tag{13}$$

In order to nondimensionalize this equation, we also define characteristic jumping velocity $v_i$ and characteristic time $\tau_i$ as

$$v_i = \sqrt{\frac{\gamma}{\rho r}}, \qquad \tau_i = \frac{\rho r^2}{\mu} \tag{14}$$

and the nondimensional velocities $v_j^*$ and $U_x^*$, nondimensional viscous dissipation time $\tau_{vis}^*$, nondimensional contact time $\tau_{cl}^*$, and nondimensional contact line length $L^*$ are given by

$$v_j^* = \frac{v_j}{v_i}, \quad U_x^* = \frac{U_x}{v_i}, \quad \tau_{vis}^* = \frac{\tau_{vis}}{\tau_i}, \quad \tau_{cl}^* = \frac{\tau_{cl}}{\tau_i}, \quad L^* = \frac{L}{r} \tag{15}$$

Therefore, eq 13 could be simplified as

$$v_j^{*2} \approx 1 - U_x^{*2}(\tau_{vis}^* + L^*\tau_{cl}^*) \tag{16}$$

Equation 16 could also be used to predict the energy conversion efficiency $\eta$ as

$$\eta \approx \frac{\frac{1}{2}v_j^2}{\frac{1}{2}mv_j^2} = v_j^{*2} \approx 1 - U_x^{*2}(\tau_{vis}^* + L^*\tau_{cl}^*) \tag{17}$$

On a flat surface, $L^*$ is equal to 2 and the time of viscous dissipation $\tau_{vis}$ and contact line dissipation $\tau_{cl}$ should be on the same order of magnitude. Thus, the prominant effect of contact line dissipation $E_{cl}$ in the nanoscale could be confirmed as

$$\frac{E_{cl}}{E_{vis}} \approx \frac{L\tau_{cl}}{r\tau_{vis}} \approx 1 \tag{18}$$

According to eq 11, the contact line length $L^*$ will become shorter with increasing nondimensional curvature $\varphi$. The average horizontal velocity $U_x^*$, contact line dissipation time $\tau_{cl}^*$, and viscous dissipation time $\tau_{vis}^*$ are inclined to decrease because of the presence of surface curvature. Therefore, we expect that the curvature-enhanced jumping could be achieved in the nanoscale as a result of the reduced viscous dissipation $E_{vis}$ and the mitigated contact line dissipation $E_{cl}$, which will be verified in the following discussion.

## 3. RESULTS AND DISCUSSION

**3.1. Dynamics of Coalescence-Induced Jumping of Nanodroplets on a Flat Surface.** To study the effects of surface curvature on droplet jumping behaviors, the dynamics of coalescence-induced nanodroplet jumping on a flat surface were first studied. The energy parameter ratio $\varepsilon_{ws}/\varepsilon_{ww}$ was set at 0.1 to model a superhydrophobic surface. The temporal evolution of the out-of-plane (vertical) centroid velocity $v_z$ of the coalescing droplet and the distance $h_{bs}$ between the lowest point of the liquid bridge and the surface are shown in Figure 2a. The snapshots of coalescence-induced jumping of nanodroplets on a flat surface are shown in Figure 2b. Similar to the



DOI: 10.1021/acs.langmuir.9b01300
Langmuir 2019, 35, 9979−9987

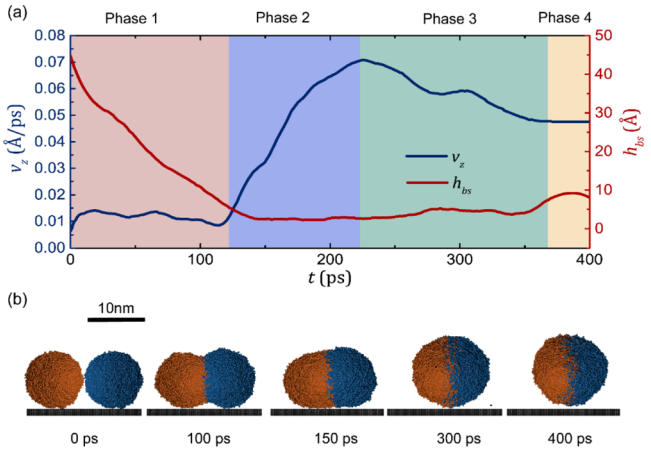


**Figure 2.** (a) Evolution of the vertical centroid velocity $v_z$ and the bridge-surface distance $h_{bs}$ during the coalescence and jumping of nanodroplets on a flat surface with $\varepsilon_{ws}/\varepsilon_{ww}$ = 0.1; (b) a series of snapshots of coalescence-induced jumping of nanodroplets on a flat surface. The two identical nanodroplets are 10 nm in diameter.

results of previous studies,[5,16,32,33] the jumping process could be divided into the following four phases.

In phase 1, the two droplets started coalescing along with the formation and growth of the liquid bridge until the evolving liquid bridge touched on the solid surface at $t$ = 120 ps. In general, the formation and expansion of the liquid bridge was believed to be surface-tension-driven and the expansion of the liquid bridge was ascribed to the negative Laplace pressure close to the center of the liquid bridge. In a more recent MD work,[34] the coalescence of two nanodroplets was found to be stochastically initiated by the thermal capillary wave on the droplet surfaces and then the as-initiated liquid bridge would expand in a faster linear regime (i.e., thermal regime) before its diameter $d_b$ exceeds the thermal length scale $l_T \approx r$.[34] Both the thermal-driven stage ($d_b \propto t$) and the surface-tension-driven stage ($d_b \propto t^{0.5}$ in inertially limited-viscous regime[15,35]) could be observed in our simulation (see Figures S1 and S2 in the Supporting Information), which could at least partly verify the validity of our simulation method.

In phase 2, the coalesced droplet accelerated upwards and its out-of-plane velocity finally reached its maximum value $v_z$ = 0.07 Å/ps at $t$ = 225 ps. As shown in Figure 2b, the beginning of acceleration is synchronized with the contact of the liquid bridge on the surface, which confirms that the bridge-impacting-induced symmetry breaking is the main driving factor of acceleration. It is regarded that the observed jumping enhancement by arranging a ridge underneath the liquid bridge[36] was essentially based on this "bridge-impacting-induced symmetry breaking" mechanism.

In phase 3, the coalesced droplet started detaching from the solid substrate whereas the out-of-plane velocity $v_z$ decelerated to a steady value ~0.05 Å/ps at $t$ = 360 ps. In phase 4, the coalesced droplet successfully detached from the surface and kept moving up with the constant velocity $v_j \approx$ 0.05 Å/ps, which is defined as the jumping velocity or launching velocity in this study. Correspondingly, the energy conversion efficiency $\eta \approx \frac{1}{2}mv_j^2/\frac{1}{2}v_i^2 \approx 0.15\%$, which is a significant reduction compared with that of ~5% in the microscale.[37] As most of the energy dissipation, including viscous dissipation and contact line dissipation, took place during the first three phases of coalescence, it is expected that energy dissipation could be mitigated if we could shrink the time span of phases 1−3.

**3.2. Dynamics of Coalescence-Induced Jumping of Nanodroplets on a Curved Surface.** Via MD simulation of coalescence of two nanodroplets on a curved surface as shown in Figure 1b, we studied the effects of surface curvature on coalescence-induced jumping of nanodroplets. In this section, the curved surface has the nondimensional curvature $\varphi$ = 2 with energy parameter ratio $\varepsilon_{ws}/\varepsilon_{ww}$ = 0.1 and the two identical nanodroplets are 10 nm in diameter as on the flat surface. The evolution of the vertical centroid velocity $v_z$ of the coalesced droplet and the evolution of the gap $h_{bs}$ between the nadir of the liquid bridge and the surface ridge (or apex) are shown in Figure 3a; and 3b illustrates the snapshots of droplet coalescence and jumping on the curved surface.

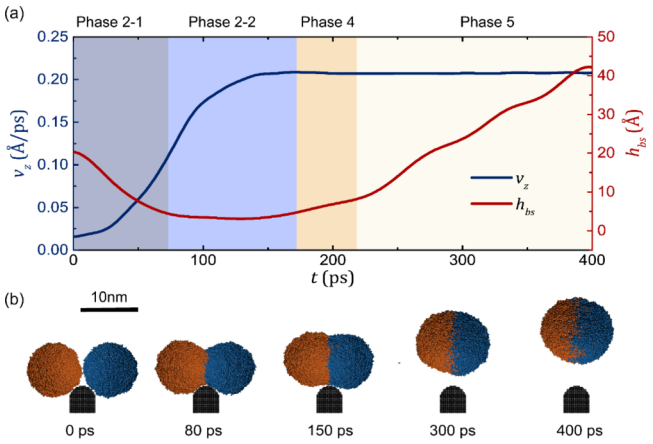


**Figure 3.** (a) Evolution of the centroid velocity $v_z$ and the bridge-surface distance $h_{bs}$ during the coalescence and jumping of nanodroplets on a curved surface with $\varphi$ = 2 and $\varepsilon_{ws}/\varepsilon_{ww}$ = 0.1; (b) a series of snapshots of coalescence-induced jumping of nanodroplets on the curved surface. The two identical nanodroplets are 10 nm in diameter.

As can be seen in Figure 3, the dynamics of the coalescence-induced nanodroplet jumping on a curved surface is distinct from that on a flat surface. On the curved surface, the coalescing droplet initiated its vertical acceleration upon the instantaneous contact of the two droplets at $t$ = 0 ps, that is, without phase 1 as observed on a flat surface. In a faster pace, the liquid bridge impinged on the surface apex as early as $t \approx$ 75 ps, implying another dominant mechanism other than the bridge-impacting-induced symmetry breaking in this phase. Here, this early jumping could be ascribed to the opposite movements of the two coalescing droplets on the curved surface. On a flat surface, the opposite and lateral movements of coalescing droplets have a relatively limited influence on their vertical jumping at least during the initial phase of coalescence. However, the lateral movements of coalescing droplets on the curved surface would lead to the instantaneous contact of droplets on the slope around the surface apex. During this impacting process, the counteractive momentum normal to the slope surface would drive the droplet jump much earlier, even before the liquid bridge gets into contact with the apex of the surface. Moreover, this early jumping might be amplified in the nanoscale because coalescing droplets in the inertial limited-viscous regime were found to behave as rigid objects.[35] From the point of view of symmetry breaking, this



DOI: 10.1021/acs.langmuir.9b01300
Langmuir 2019, 35, 9979−9987

early jumping could be attributed to the early symmetry breaking caused by the translation of the coalescing droplets, that is, "lateral-motion-enhanced symmetry breaking". Once the liquid bridge impinges on the apex of the curved surface, the coalescing droplet will also be simultaneously accelerated by the "bridge-impingement-induced symmetry breaking", which is confirmed by the steeper ramp of the vertical centroid velocity $v_z$ at $t \approx 75$ ps. Therefore, unlike phase 2 on a flat surface, the acceleration process on the curved surface could be divided into two subphases, that is, phase 2-1 during which only lateral-motion-enhanced early symmetry breaking is dominant before the liquid bridge impacts on the surface; and phase 2-2 whereas both the lateral-motion-induced early symmetry breaking and the bridge-impingement-induced symmetry breaking exert joint effects on the acceleration of the coalescing droplet.

Following the acceleration phase, the coalescing droplet reached its maximum velocity at $t = 170$ ps and was about to detach from the surface. However, on the curved surface, there is no deceleration process as phase 3 on a flat surface. To explain this phenomenon, we compared the evolution of solid−liquid molecules $N_{ls}^*$ on both the flat surface and the curved surface as shown in Figure 4. Here, the nondimensional

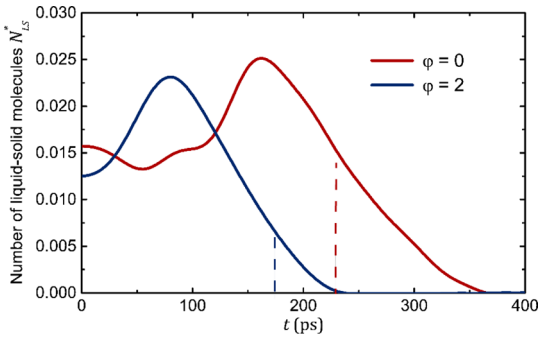


**Figure 4.** Effect of surface curvature $\varphi$ on the evolution of liquid−solid molecules $N_{ls}^*$ during the coalescence-induced jumping process. The red and navy dashed lines denote the ends of phase 2 on the flat surface and the curved surface, respectively.

number of solid−liquid molecules $N_{ls}^* = N_{ls}/N_0$, that is, the ratio of the number of water molecules $N_{ls}$ within the cutoff distance of the solid substrate to the overall water molecules $N_0$ in the simulation system. It is rational to use the values of solid−liquid molecules $N_{ls}^*$ to predict the evolution of adhesion force. Comparing with $N_{ls}^*$ on the flat surface, the peak value of $N_{ls}^*$ on the curved surface arose much earlier ($t = 77$ ps on the curved surface vs $t = 162$ ps on the flat surface) and the relatively less solid−liquid molecules $N_{ls}^*$ at the end of phase of 2-2 (see the dashed lines in Figure 4) led to the significant reduction of adhesion force during the detachment phase. On the other hand, the occurrence of the peak value of contact line length is anteceded on the curved surface than that on a flat surface, leading to the depressed contact line dissipation during the detachment process. Consequently, sharply contrary to that on a flat surface, coalescing on a curved surface exhibits no apparent deceleration process. Besides, as shown in Figure 4, both the initial and peak values of solid−liquid molecules $N_{ls}^*$ only vary slightly with respect to $\varphi$, indicating that the change of surface energy of a droplet on curved surfaces in the energy analysis of section 2.2 could be ignored.

Without the deceleration process as phase 3 on a flat surface, the droplet jumped off the curved surface with its maximum velocity. The final jumping velocity $v_j$ is increased from ∼0.05 Å/ps on a flat surface to 0.20 Å/ps on the curved surface; the corresponding energy conversion efficiency $\eta$ is improved by ∼20 times from 0.15% on a flat surface to 2.9% on the curved surface. Note that it only took about half the amount of time for the jumping droplet on the curved surface to reach the same height in comparison to that on the flat surface, that is, 215 ps versus 400 ps. In this way, the time span of phases 2-1 and 2-2 on the curved surface, corresponding to phases 1−3 on a flat surface, has been dramatically decreased.

**3.3. Effects of Surface Curvature on Jumping Velocity.** To comprehensively investigate the effects of surface curvature on the jumping behaviors of nanodroplets, we further simulated the coalescence-induced jumping of nanodroplets on surfaces with different curvatures ($\varphi = 0.25, 1, 2$) whereas the surface wettability is fixed at $\varepsilon_{ws}/\varepsilon_{ww} = 0.1$. The evolution of the instantaneous vertical centroid velocity $v_z$ and the centroid height of droplet $z_j$ are depicted in Figure 5.

It can be seen that jumping behaviors of droplets strongly depend on surface curvature $\varphi$. With the increase of surface curvature from $\varphi = 0$ to $\varphi = 2$, the droplets could jump off the surface with higher velocities and reach higher heights within the same period of 400 ps. Although the four curves in Figure 5b are qualitatively similar, the gradual disappearance of phase 1 and phase 3 with increasing $\varphi$ could be clearly perceived. In Figure 5c, the final jumping velocities $v_j^*$ increase with increasing surface curvature $\varphi$, indicating that enhanced surface curvature $\varphi$ could be utilized to significantly promote the coalescence-induced droplet jumping at least in the nanoscale. However, if surface curvature $\varphi$ rises to an even higher degree, this jumping enhancement effect would be eventually diminished as a result of the almost no solid−liquid contact for a sufficiently small curvature radius ($\varphi \gg 2$). Thus, a critical value of $\varphi$ might exist, only below which the early jumping because of "lateral-motion-enhanced symmetry breaking" could occur and above which the jumping behavior of the coalesced droplet would be similar to that on surfaces with ridge/roughness.[17] However, it is anticipated that this critical value should be very large as the curvature-induced jumping enhancement still works for the case of $\varphi = 20$ in the microscale.[20] Therefore, we restricted our MD simulation in the range of $\varphi \leq 2$ given the limited computation resources and the subatomic discreteness of the gold substrate.

According to eq 17, this enhanced jumping of the coalesced droplet implies that viscous dissipation and contact line dissipation might be mitigated because of the existence of surface curvature. To find the evolution of viscous dissipation $E_{vis}$, instantaneous lateral velocity $v_x$ for different curvatures were extracted from our MD simulation. As illustrated in Figure 5d, the coalescing droplets in all cases began horizontal acceleration at $t = 0$ ps, and the lateral velocity $v_x$ reached the maximum values at $t \approx 50$ ps, then gradually damped to $v_x = 0$ at $t \approx 400$ ps.

The almost identical profiles in Figure 5d indicate that both $U_x^*$ (∼0.05) and $\tau_{vis}^*$(∼14.29) were almost unchanged for the four jumping cases on different curvatures. According to eq 9, viscous dissipation $E_{vis}$ can be taken as a constant and the reduction of energy dissipation on curved surfaces can only be ascribed to the reduction of contact line dissipation $E_{cl}$. Thus, eq 17 could be simplified as



DOI: 10.1021/acs.langmuir.9b01300
Langmuir 2019, 35, 9979−9987

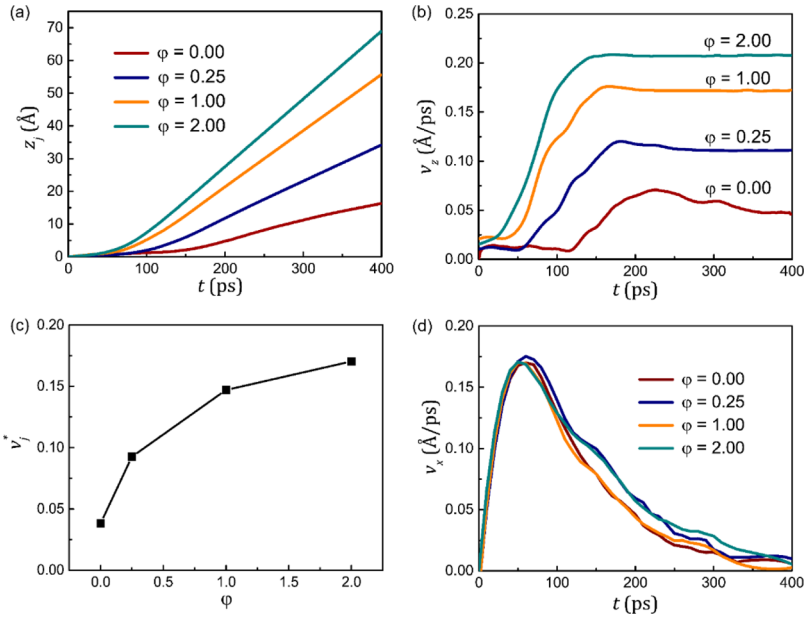


**Figure 5.** (a) Effect of surface curvature $\varphi$ on the evolution of droplet centroid height $z_j$; (b) effect of surface curvature $\varphi$ on the evolution of vertical centroid velocity $v_z$ of nanodroplets. (c) Nondimensional jumping velocity of droplets on superhydrophobic surfaces with different curvatures. (d) Evolution of the horizontal coalescence velocity $v_x$ during the coalescence of nanodroplets on surfaces with different curvatures. The surface wettability is maintained at $\varepsilon_{ws}/\varepsilon_{ww} = 0.1$.

$$\eta \approx C_1 - C_2\tau_{cl}^* L^* \tag{19}$$

where $C_1$ and $C_2$ are constant factors. Equation 19 implies that surface curvature can improve the energy conversion efficiency via reducing both the contact line length $L^*$ and contact time $\tau_{cl}^*$. Indeed, Figure 6 reveals a linear relationship between the

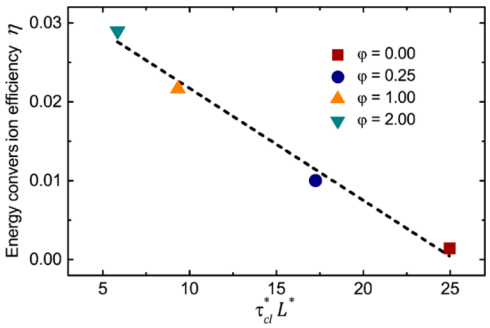


**Figure 6.** Energy conversion efficiency $\eta$ on surfaces with different curvatures follow a linear relationship with $\tau_{cl}^* L^*$, that is, the product of contact line length and contact time. The surface wettability is maintained at $\varepsilon_{ws}/\varepsilon_{ww} = 0.1$.

energy conversion efficiency $\eta$ and $\tau_{cl}^* L^*$, which is in line with the prediction of eq 19. On the basis of our simulation results, the contact time $\tau_{cl}^*$ could be greatly shortened on the curved surface because of the early jumping and weaker deceleration, that is, the disappearance of phase 1 and phase 3 on the curved surface as shown in Figure 3a. Also, the contact line length $L^*$ could be decreased with increasing $\varphi$ according to eq 11. Therefore, this significant improvement of energy conversion efficiency $\eta$ could be explained by the negative linear relationship between $\eta$ and $\tau_{cl}^* L^*$. Furthermore, this scaling analysis also implies that it is the reduction of contact line dissipation $E_{cl}$ rather than viscous dissipation $E_{vis}$ which plays the dominant role in enabling nanodroplet jumping with higher energy conversion efficiency $\eta$ on curved surfaces.

Although the droplet size $r$ is fixed and only surface curvature $(1/R)$ is varied in our MD simulations, the conclusions based on the nondimensional analysis should be still valid for droplets with varying sizes on a curvature-fixed surface. For instance, regarding dropwise condensation on a nanostructured surface, the nanoembryos would keep growing before coalescing with neighboring nanoembryos, resulting in an effective increase of surface curvature $\varphi$ as well. According to our analysis, the energy conversion efficiency $\eta$ could be improved via increasing the nondimensional curvature $\varphi$. Only when $\varphi$ goes beyond a critical value $\varphi_c$ could the coalesced embryos successfully jump off the surface with sufficient kinetic energy (the value of these critical nondimensional curvatures $\varphi_c$ could be found in the next section). Correspondingly, on a surface with a fixed curvature $(1/R)$, a critical radius $r_c$ of nanoembryos should exist, above which the energy barrier for successful jumping could be overcome. In fact, a similar critical radius $r_c$ has been experimentally observed during the detachment of condensate droplet from a rounded fiber in the microscale.[38] More importantly, once $\varphi_c$ becomes fixed for surfaces with constant surface wettability and droplets have specific physical properties (viscosity, surface tension, etc.), the only way to reduce the critical radius $r_c$ is to increase surface curvature $(1/R)$. In other words, a higher surface curvature $(1/R)$ could promote the coalescence-induced jumping during the earlier life of condensate embryos. From the point of view of practical applications, increasing the surface curvature by introducing nanoroughness on an engineered surface would lead to the jumping removal of condensate embryos during the very beginning of their formation, which could be utilized in designing advanced functional surfaces (self-cleaning surface, anti-icing surface, etc.) with much delayed condensate flooding or remarkably depressed ice/contaminants adhesion.



DOI: 10.1021/acs.langmuir.9b01300
Langmuir 2019, 35, 9979−9987

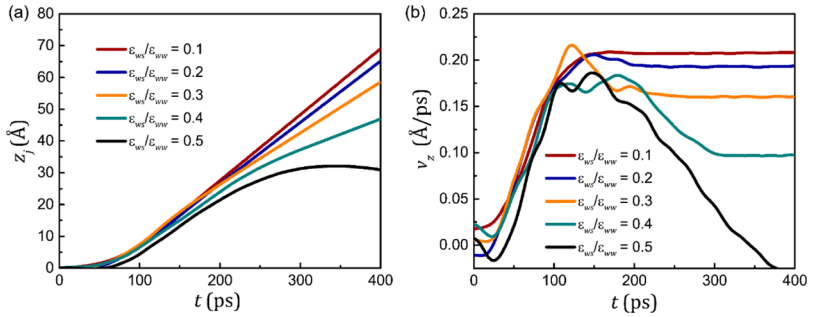


**Figure 7.** Effects of surface wettability on the evolutions of (a) droplet centroid height $z_j$ on a curved surface of $\varphi = 2$; (b) vertical centroid velocity $v_z$ of nanodroplets on a curved surface of $\varphi = 2$.

**3.4. Effect of Surface Wettability on Coalescence-Induced Jumping on Curved Surfaces.** As the curved structures could enhance coalescence-induced jumping on a superhydrophobic surface, we hope such enhancement effect could prevail on surfaces with a wider range of wettability. Thus, by varying the energy parameter ratio of the O−O interaction to the O−Au interaction $\varepsilon_{ws}/\varepsilon_{ww}$ from 0.1 to 0.5, the effect of surface wettability on the coalescence-induced jumping of nanodroplets was investigated on a nanofiber with a fixed curvature $\varphi = 2$. Figure 7a,b show the temporal evolution of the centroid height $z_j$ and the vertical centroid velocity $v_z$, respectively, for nanodroplet jumping on the curved surfaces with different wettabilities.

As shown in Figure 7a,b, on the curved surface with increasing surface wettability, the coalesced droplet would garner a decreasing jumping velocity, reaches a lower height within 400 ps, and even fails to jump when $\varepsilon_{ws}/\varepsilon_{ww} = 0.5$. This decreasing jumping velocity could be explained by the following two reasons. First, on the surface with higher wettability, the stronger attractive force between water molecules and the substrate atoms would prohibit the droplet from jumping off the surface with a higher velocity. The failure case of $\varepsilon_{ws}/\varepsilon_{ww} = 0.5$ could be attributed to the stronger adhesion work $E_a$, which cannot be neglected on the less superhydrophobic surface. Second, with the increase of surface wettability, it apparently takes a longer time for a droplet to wet and to detach from the surface, which means the contact time $\tau_{cl}^*$ is inevitably increased. Meanwhile, the contact line $L^*$ will also be increased because of the increasing contact area.[39] Owing to the increase of contact line $L^*$ and contact time $\tau_{cl}^*$, more surface energy will be dissipated via contact line dissipation $E_{cl}$. Consequently, stronger adhesion work $E_a$ and more contact line dissipation $E_{cl}$ may jointly result in energy-ineffective jumping or even no jumping.

On the basis of the MD simulations, we plot out a phase map as shown in Figure 8 for 20 coalescence cases with different surface curvatures $\varphi$ and surface wettability $\varepsilon_{ws}/\varepsilon_{ww}$, where green rounded points denote the cases that coalesced droplets could successfully jump off the surface and the red square points denote the failed cases. As mentioned in section 3.4, the critical nondimensional curvatures $\varphi_c$ of successful jumping for different surface wettabilities could be found in Figure 8. It is reasonable that $\varphi_c$ is dependent of surface wettability ($\varepsilon_{ws}/\varepsilon_{ww}$) because a higher surface curvature is required for successful jumping on a more wettable surface. Furthermore, this phase map shows that the threshold of hydrophobicity for successful jumping is reduced via increasing surface curvature $\varphi$. Nanodroplet jumping becomes possible on a less superhydrophobic surface ($\varepsilon_{ws}/\varepsilon_{ww} = 0.4$) if surface

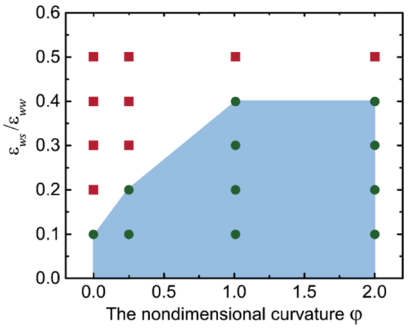


**Figure 8.** Phase map of coalescence-induced jumping in terms of surface curvature ratio and surface wettability.

curvature $\varphi > 1$. Thus, adjusting the surface curvature turns out to be an effective method to enhance droplet jumping in the nanoscale.

As discussed in the introduction, some of previous studies have made tremendous efforts to enhance coalescence-induced jumping on structured superhydrophobic surfaces.[17−21] One of these methods is to integrate a single micro/nanoridge under the liquid bridge so that the early-contact between the liquid bridge and the surface ridge would improve the energy conversion efficiency.[17−19] Similar to these designs, increasing surface roughness curvature can effectively facilitate the bridge-impingement-induced symmetry breaking as we discussed before. Importantly, the curvature-induced enhancement has two advantages that the other methods do not have. First, for the flat surface with micro/nanoridges, the enhancement effect of the ridge would be maximized when the ridge structure is arranged underneath the liquid bridge between two coalescing droplets. However, on a curved surface, droplets' positions are not specifically required because both the bridge-impingement-induced early symmetry breaking and the lateral-motion-enhanced symmetry breaking could take synergistic effect everywhere on the curved structures like nanowires and nanofibers. Second, as a previous study pointed out,[19] the existence of macrotexture ridges would increase the liquid−solid interface and additional surface energy can be stored in the deformed droplet, which eventually leads to the improved energy conversion efficiency. However, the incurred increase of solid (ridge)−liquid contact area during the detachment phase would limit this method only on nonwetting surfaces with ultrahigh contact angles so that the effect of adhesion force could be depressed. In contrast, the liquid−solid contact area on curved surfaces has only slight changes as evidenced in Figure 4, that is, the maximum number of liquid−solid molecules on the curved surfaces is almost equal to that on the



DOI: 10.1021/acs.langmuir.9b01300
Langmuir 2019, 35, 9979−9987

flat surface. In this scenario, the adhesion force is not an additional prohibitive factor for effective coalescence-induced jumping. Moreover, the intrinsic surface curvatures prevailing in nature should be more complex (e.g., surface curvatures might exist in three dimensions) rather than the two-dimensional surface curvature in our modeling, which might further enhance the jumping behavior of nanodroplets. In addition, the asymmetric curvature of nanofibers might affect the jumping direction of small droplets, which has been observed in a recent experimental study in the microscale.[37] In short, compared with the design of a flat surface with micro/nanoridges, the surface curvature-enhanced jumping moderates the demanding requirements on surface superhydrophobicity and the specific spatial arrangement of droplets, shedding light on integrating advanced micro/nanostructures on engineered surfaces for practical applications.

## 4. CONCLUSIONS

In this work, we investigated the coalescence-induced jumping of nanodroplets on curved surfaces by MD simulations. First, the study of droplet jumping dynamics on curved surfaces shows that the onset of jumping on a curved surface is antedated and coalesced droplets jump off the surface with a higher velocity within a shorter period. By varying the surface curvature from $\varphi = 0$ to $\varphi = 2$, we demonstrated that surface curvature could improve the energy conversion efficiency of coalescence-induced jumping by about 20 times. To explain this curvature-enhanced jumping in the nanoscale, energy-based scaling analysis was performed to identify the significance of contact line dissipation in nanoscale energy conversion. Specifically, the almost independent coalescence time and the lumped lateral velocity for different surface curvatures imply that the reduction of contact line dissipation should be the underlying mechanism of curvature-enhanced jumping in the nanoscale. Finally, the effect of surface wettability on coalescence-induced jumping on curved surfaces was investigated to generate a phase diagram, presenting the threshold of surface superhydrophobicity for successful jumping on curved surfaces with different wettabilities. It is found that curvature-induced jumping enhancement could occur on a less superhydrophobic surface if the surface curvature $\varphi > 1$. Thus, we envision this curvature-enhanced jumping could be utilized in a wider range of practical applications because of its less strict demands on droplets' positions and surface superhydrophobicity. Furthermore, the paradigm of curved surfaces in this MD study actually characterizes the surface topography with roughness on the nanoscale or microscale, on which coalescence-induced droplet jumping has been experimentally observed. We believe our study of curvature-enhanced jumping of nanodroplets offers new insights into nanodroplet behaviors especially on nanostructured morphology.

## ■ ASSOCIATED CONTENT

### Supporting Information

The Supporting Information is available free of charge on the ACS Publications website at DOI: 10.1021/acs.langmuir.9b01300.

Dynamics of droplet coalescence in the thermal-driven regime and the surface-tension-driven regime; the contact angles on a flat surface with different energy parameter ratios $\varepsilon_{ws}/\varepsilon_{ww}$ (PDF)

Coalescence-induced jumping of two nanodroplets with a diameter of 10 nm on a flat surface and the successful detachment of the coalesced droplet from the surface ($\varepsilon_{ws}/\varepsilon_{ww} = 0.1$) (MP4)

Coalescence-induced jumping of two nanodroplets with a diameter of 10 nm on a curved surface ($\varphi = 2$, $\varepsilon_{ws}/\varepsilon_{ww} = 0.1$) (MP4)

A failure case where no jumping occurs on a curved surface with less superhydrophobicity ($\varphi = 2$, $\varepsilon_{ws}/\varepsilon_{ww} = 0.5$) (MP4)

## ■ AUTHOR INFORMATION


### Corresponding Author

*E-mail: chengjt@vt.edu. Phone: (540) 231-4164. Fax: (540) 231-9100.

### ORCID

Jiangtao Cheng: 0000-0002-0897-3937


### Author Contributions

†X.H. and L.Z. contributed equally to this work.

### Notes

The authors declare no competing financial interest.

## ■ ACKNOWLEDGMENTS

This work is financially supported by NSF CBET under grant number 1550299, NSF ECCS under grant number 1808931, and Institute for Critical Technology and Applied Science at Virginia Tech. The authors also acknowledge Advanced Research Computing at Virginia Tech for providing computational resources and technical support to this work.

## ■ REFERENCES


(1) Chen, C.-H.; Cai, Q.; Tsai, C.; Chen, C.-L.; Xiong, G.; Yu, Y.; Ren, Z. Dropwise condensation on superhydrophobic surfaces with two-tier roughness. *Appl. Phys. Lett.* **2007**, *90*, 173108.

(2) Boreyko, J. B.; Chen, C.-H. Self-propelled dropwise condensate on superhydrophobic surfaces. *Phys. Rev. Lett.* **2009**, *103*, 184501.

(3) Wisdom, K. M.; Watson, J. A.; Qu, X.; Liu, F.; Watson, G. S.; Chen, C.-H. Self-cleaning of superhydrophobic surfaces by self-propelled jumping condensate. *Proc. Natl. Acad. Sci. U.S.A.* **2013**, *110*, 7992−7997.

(4) Enright, R.; Miljkovic, N.; Sprittles, J.; Nolan, K.; Mitchell, R.; Wang, E. N. How Coalescing Droplets Jump. *ACS Nano* **2014**, *8*, 10352−10362.

(5) Liu, F.; Ghigliotti, G.; Feng, J. J.; Chen, C.-H. Numerical simulations of self-propelled jumping upon drop coalescence on non-wetting surfaces. *J. Fluid Mech.* **2014**, *752*, 39−65.

(6) Miljkovic, N.; Enright, R.; Nam, Y.; Lopez, K.; Dou, N.; Sack, J.; Wang, E. N. Jumping-droplet-enhanced condensation on scalable superhydrophobic nanostructured surfaces. *Nano Lett.* **2012**, *13*, 179−187.

(7) Lv, C.; Hao, P.; Yao, Z.; Niu, F. Departure of condensation droplets on superhydrophobic surfaces. *Langmuir* **2015**, *31*, 2414−2420.

(8) Lv, J.; Song, Y.; Jiang, L.; Wang, J. Bio-inspired strategies for anti-icing. *ACS Nano* **2014**, *8*, 3152−3169.

(9) Zhang, Q.; He, M.; Chen, J.; Wang, J.; Song, Y.; Jiang, L. Anti-icing surfaces based on enhanced self-propelled jumping of condensed water microdroplets. *Chem. Commun.* **2013**, *49*, 4516−4518.

(10) Miljkovic, N.; Preston, D. J.; Enright, R.; Wang, E. N. Jumping-droplet electrostatic energy harvesting. *Appl. Phys. Lett.* **2014**, *105*, 013111.

(11) Miljkovic, N.; Preston, D. J.; Enright, R.; Wang, E. N. Electrostatic charging of jumping droplets. *Nat. Commun.* **2013**, *4*, 2517.




DOI: 10.1021/acs.langmuir.9b01300
*Langmuir* 2019, 35, 9979−9987

(12) Cha, H.; Xu, C. Y.; Sotelo, J.; Chun, J. M.; Yokoyama, Y.; Enright, R.; Miljkovic, N. Coalescence-induced nanodroplet jumping. *Phys. Rev. Fluids* **2016**, *1*, 064102.
(13) Wang, F.-C.; Yang, F.; Zhao, Y.-P. Size effect on the coalescence-induced self-propelled droplet. *Appl. Phys. Lett.* **2011**, *98*, 053112.
(14) Liang, Z.; Keblinski, P. Coalescence-induced jumping of nanoscale droplets on super-hydrophobic surfaces. *Appl. Phys. Lett.* **2015**, *107*, 143105.
(15) Gao, S.; Liao, Q.; Liu, W.; Liu, Z. Coalescence-Induced Jumping of Nanodroplets on Textured Surfaces. *J. Phys. Chem. Lett.* **2018**, *9*, 13−18.
(16) Xie, F.-F.; Lu, G.; Wang, X.-D.; Wang, B.-B. Coalescence-Induced Jumping of Two Unequal-Sized Nanodroplets. *Langmuir* **2018**, *34*, 2734−2740.
(17) Xie, F.-F.; Lu, G.; Wang, X.-D.; Wang, D.-Q. Enhancement of Coalescence-Induced Nanodroplet Jumping on Superhydrophobic Surfaces. *Langmuir* **2018**, *34*, 11195−11203.
(18) Wang, K.; Liang, Q.; Jiang, R.; Zheng, Y.; Lan, Z.; Ma, X. Self-enhancement of droplet jumping velocity: the interaction of liquid bridge and surface texture. *RSC Adv.* **2016**, *6*, 99314−99321.
(19) Vahabi, H.; Wang, W.; Mabry, J. M.; Kota, A. K. Coalescence-induced jumping of droplets on superomniphobic surfaces with macrotexture. *Sci. Adv.* **2018**, *4*, No. eaau3488.
(20) Zhang, K.; Liu, F.; Williams, A. J.; Qu, X.; Feng, J. J.; Chen, C.-H. Self-Propelled Droplet Removal from Hydrophobic Fiber-Based Coalescers. *Phys. Rev. Lett.* **2015**, *115*, 074502.
(21) Huang, J.-J.; Xiao, X.-B.; Li, Y.-J. Numerical Investigation of Coalescence-Induced Droplet Jumping from a Hydrophobic Fiber. *Langmuir* **2018**, *34*, 14186−14195.
(22) Li, B.; Xin, F.; Tan, W.; Zhu, G. A New Theoretical Model for Coalescence-Induced Droplet Jumping on Hydrophobic Fibers. *Ind. Eng. Chem. Res.* **2018**, *57*, 8299−8307.
(23) Carlson, A.; Bellani, G.; Amberg, G. Contact line dissipation in short-time dynamic wetting. *Europhys. Lett.* **2012**, *97*, 44004.
(24) Zhao, L.; Cheng, J. The mechanism and universal scaling law of the contact line friction for the Cassie-state droplets on nano-structured ultrahydrophobic surfaces. *Nanoscale* **2018**, *10*, 6426−6436.
(25) Johansson, P.; Hess, B. Molecular origin of contact line friction in dynamic wetting. *Phys. Rev. Fluids* **2018**, *3*, 074201.
(26) Plimpton, S. Fast parallel algorithms for short-range molecular dynamics. *J. Comput. Phys.* **1995**, *117*, 1−19.
(27) Hockney, R.; Eastwood, J. *Computer Simulation Using Particles*; Adam Hilger: New York, 1989.
(28) Vandadi, A.; Zhao, L.; Cheng, J. Resistant energy analysis of self-pulling process during dropwise condensation on superhydrophobic surfaces. *Nanoscale Adv.* **2019**, *1*, 1136−1147.
(29) Zhao, L.; Cheng, J. Analyzing the molecular kinetics of water spreading on hydrophobic surfaces via molecular dynamics simulation. *Sci. Rep.* **2017**, *7*, 10880.
(30) de Ruijter, M. J.; De Coninck, J.; Oshanin, G. Droplet spreading: Partial wetting regime revisited. *Langmuir* **1999**, *15*, 2209−2216.
(31) Li, H.; Paneru, M.; Sedev, R.; Ralston, J. Dynamic Electrowetting and Dewetting of Ionic Liquids at a Hydrophobic Solid-Liquid Interface. *Langmuir* **2013**, *29*, 2631−2639.
(32) Wang, Y.; Ming, P. Effect of radius ratios of two droplets on coalescence-induced self-propelled jumping. *AIP Adv.* **2018**, *8*, 065320.
(33) Farokhirad, S.; Morris, J. F.; Lee, T. Coalescence-induced jumping of droplet: Inertia and viscosity effects. *Phys. Fluids* **2015**, *27*, 102102.
(34) Perumanath, S.; Borg, M. K.; Chubynsky, M. V.; Sprittles, J. E.; Reese, J. M. Droplet Coalescence is Initiated by Thermal Motion. *Phys. Rev. Lett.* **2019**, *122*, 104501.
(35) Paulsen, J. D.; Burton, J. C.; Nagel, S. R.; Appathurai, S.; Harris, M. T.; Basaran, O. A. The inexorable resistance of inertia determines the initial regime of drop coalescence. *Proc. Natl. Acad. Sci. U.S.A.* **2012**, *109*, 6857−6861.
(36) Abolghasemibizaki, M.; Mohammadi, R. Droplet impact on superhydrophobic surfaces fully decorated with cylindrical macro-textures. *J. Colloid Interface Sci.* **2018**, *509*, 422−431.
(37) Yan, X.; Zhang, L.; Sett, S.; Feng, L.; Zhao, C.; Huang, Z.; Vahabi, H.; Kota, A. K.; Chen, F.; Miljkovic, N. Droplet Jumping: Effects of Droplet Size, Surface Structure, Pinning, and Liquid Properties. *ACS Nano* **2019**, *13*, 1309−1323.
(38) Lorenceau, É.; Clanet, C.; Quéré, D. Capturing drops with a thin fiber. *J. Colloid Interface Sci.* **2004**, *279*, 192−197.
(39) Blake, T. D.; Clarke, A.; De Coninck, J.; de Ruijter, M. J. Contact Angle Relaxation during Droplet Spreading: Comparison between Molecular Kinetic Theory and Molecular Dynamics. *Langmuir* **1997**, *13*, 2164−2166.


DOI: 10.1021/acs.langmuir.9b01300
*Langmuir* 2019, 35, 9979−9987